JMEPEG (2012) 21:2090–2098
DOI: 10.1007/s11665-012-0134-2

1059-9495/$19.00

Influence of Processing Parameters on Residual Stress of High Velocity Oxy-Fuel Thermally Sprayed WC-Co-Cr Coating

M. Gui, R. Eybel, B. Asselin, S. Radhakrishnan, and J. Cerps

(Submitted November 26, 2010; Accepted: 7 November 2011)

Residual stress in high velocity oxy-fuel (HVOF) thermally sprayed WC-10Co-4Cr coating was studied based on design of experiment (DOE) with five factors of oxygen flow, fuel gas hydrogen flow, powder feed rate, stand-off distance, and surface speed of substrate. In each DOE run, the velocity and temperature of in-flight particle in flame, and substrate temperature were measured. Almen-type N strips were coated, and their deflections after coating were used for evaluation of residual stress level in the coating. The residual stress in the coating obtained in all DOE runs is compressive. In the present case of HVOF thermally sprayed coating, the residual stress is determined by three types of stress: peening, quenching, and cooling stress generated during spraying or post spraying. The contribution of each type stress to the final compressive residual stress in the coating depends on material properties of coating and substrate, velocity and temperature of in-flight particle, and substrate temperature. It is found that stand-off distance is the most important factor to affect the final residual stress in the coating, following by two-factor interaction of oxygen flow and hydrogen flow. At low level of stand-off distance, higher velocity of in-flight particle in flame and higher substrate temperature post spraying generate more peening stress and cooling stress, resulting in higher compressive residual stress in the coating.

Keywords design of experiment, HVOF thermal spray, processing parameters, residual stress, tungsten carbide coating

1. Introduction

Tungsten carbide cobalt-based coatings produced by high velocity oxy-fuel (HVOF) thermal spray have been used on aviation engine and airframe components, such as landing gear and actuator. HVOF-sprayed WC-Co coatings demonstrate adequate fatigue and corrosion properties and superior wear resistance in comparison with hard chrome plating. Hence, the coatings have increasingly become an alternative to hard chrome plating (Ref 1-4).

For HVOF-sprayed WC-Co coatings, considerable effort has been devoted to study their microstructure, wear, and mechanical properties (Ref 5-11). Residual stress in a coating is one major factor to relate to the performance of the coating and substrate being used. A compressive residual stress in a coating can enhance resistance to fatigue fracture and stress corrosion cracking of the coating. This will be more important if the coated part is used in fatigue critical environment, such as landing gear component. Various methods have been employed to measure residual stress in thermally sprayed coatings, such as x-ray diffraction (Ref 11, 12), hole drilling (Ref 13), Almen strip deflection (Ref 14-16), and in-situ curvature measurement technique, developed more recently (Ref 17, 18). Industrially, Almen strip deflection has been used for evaluating residual stress in a HVOF coating, and become a simple method for coating quality control to assess whether the level of residual stress in the coating meets a requirement. In some applications of WC-Co coatings, a compressive residual stress in the coatings is mandatory. For example, per AMS 2448 (Aerospace Material Specification), HVOF-sprayed WC-Co coatings have to demonstrate a compressive residual stress with a value between +0.003 and +0.012 inches (0.076-0.30 mm) of deflection of Almen-type N strip after it is coated to 0.005-in. (0.127-mm) thickness.

It has been found that spray parameters, such as powder feed rate (FR) and stand-off distance, as well as coating thickness, affect on the residual stress in HVOF-sprayed WC-Co coatings (Ref 14-16). However, the relevant studies in this area are still limited. In this study, the residual stress in HVOF-sprayed WC-10Co-4Cr coating was investigated using Almen strip deflection method. Design of experiment (DOE) methodology was employed to organize experiments and analyze experimental data. Spray runs were conducted with an industrial thermal spray facility. The influence of HVOF spray parameters on the residual stress in the coating was described statistically, and discussed based on temperature and velocity of in-flight particle in flame and substrate temperature.

2. Experimental Procedures

2.1 High Velocity Oxy-Fuel Facility, Materials, and Methods

A Jet Kote III HVOF system from Stellite Coatings, equipped with a Computer Integrated Thermal Spray (CITS)

M. Gui, B. Asselin, S. Radhakrishnan, and **J. Cerps**, Department of Manufacturing Engineering, Messier-Dowty Inc., Toronto, ON, Canada; and **R. Eybel**, Department of Materials and Process, Messier-Dowty Inc., Toronto, ON, Canada. Contact e-mail: manchangg@hotmail.com.

control system provided by Progressive Technologies, was used for coating spray. HVOF torch, JK3000, was manipulated by a FANUC M-710iB robot. Hydrogen and nitrogen were used as fuel and carrier gas, respectively. Feedstock used is Stellite product of JK120H, an agglomerated and sintered 86 wt.% WC-10 wt.% Co-4 wt.% Cr powder, with a single production lot for all DOE runs. This type of powder has been extensively used to make coating on landing gear parts. The size distribution of the powder used is shown in Table 1.

Standard Almen-type N strips with the size of $76 \times 19 \times 0.8$ mm were HVOF coated for evaluating residual stress in the coating. The Almen strips were grit blasted on both sides to minimize curvature of the strips to less than 0.025-mm arc height before coating. Grit-blasted Almen strips were mounted on a drum fixture (cylinder) by four screws with location as indicated in specification of SAE J442 with the convex surface of the Almen strips in the up position. The drum fixture was particularly designed for coating production qualification test, in which four types of specimens for microstructure, bond strength, bend test, and residual stress (Almen strip) were mounted and coated at a single spray run. HVOF torch traversed Almen strip lengthwise during spraying. Three Almen strips were coated in each spray run. The average of their measurements was taken as test result. Arc height of Almen strip was measured by Almen gauge specified in SAE J442, with a resolution of 0.0025 mm. The net deflection of Almen strip, i.e., the change of arc height of Almen strip after and before coating, is used to represent the residual stress in the coating. Almen strip in each spray run was targeted to be coated to 0.127-mm (0.005-in.) thickness. Actual thickness of coating in all spray runs varied from 0.114 to 0.152 mm and was measured by a flat anvil micrometer. Because the residual stress of the coating is varied with the coating thickness, all test results were finally normalized to a 0.127-mm coating thickness by the way described in the literature (Ref 14). The relationship between deflection of Almen strip and average residual stress in a coating can be approximately described by (Ref 19):

$$\sigma = -E_c Y/R \qquad \text{(Eq 1)}$$

where σ is the average residual stress, Y is the neutral axis of the coated strip, R is the curvature radius of Almen strip, and E_c the Young's modulus of the coating. The bigger the deflection of Almen strip, the smaller the value of R, and hence, a higher residual stress exists in the coating.

The temperature of drum fixture (substrate) during spraying process was measured by a Raytek infrared pyrometer device. The highest temperature detected in each spray run was recorded as the substrate temperature, and it usually happened at the end of Almen strip-spraying cycle. Temperature and velocity of in-flight particle in flame were measured by an Accuraspray G3 device at the beginning and the end of each spray run for 2-3 min after the flame was stabilized. The readings were saved on file, and the average value was used as the final measurement result. The G3 device was set up at a unique distance of 152 mm (6 in.) from nozzle to lens in all DOE runs. HVOF spray system and all measurement tools and devices used were calibrated.

Table 1 Particle Size of WC-Co-Cr Powder Used for HVOF Spraying

Particle size, μm	Vol.%
44-66	3
22-44	63
11-22	27
<11	Balance

2.2 DOE for Spraying Process

High velocity oxy-fuel is a complicated process. Many process variables may impact coating properties. However, based on our experience and importance for production, five major process variables of oxygen flow, hydrogen fuel gas flow, powder FR, stand-off distance from nozzle to substrate, and surface speed (SFM) of substrate were taken as factors in the present DOE. The responses considered in the DOE include microstructure (oxide/pore level), micro-hardness, deposition rate, and residual stress of the coating, but only the last one will be discussed in this study. An ordinary experimental design is one with each factor setting at two levels (low and high). In the current case, if all possible low/high combinations of five factors are conducted, then there will be total 32 runs. In order to reduce experimental run, two-level fractional factorial design, 2_V^{5-1}, was used, and a total of 16 experiments were performed. In this design, no main effects are aliased with two-factor interactions, but two-factor interactions are confounded with three or more factor interaction. Two level settings of five factors are listed in Table 2. The details of 16 DOE spray runs in standard order are shown in Table 3. Actual spray run was randomized. In DOE runs, torch traverse speed, inch per minute, is taken as 0.1× rpm (rotation speed of substrate,

Table 2 Setting of factors and two levels for DOE of HVOF coating

Factor	Low (−1)	High (+1)
Oxygen flow, SCFH	570	650
Hydrogen flow, SCFH	1330	1430
Powder FR, G/min	28	48
Stand-off distance, mm	152	203
SFM, m/min	61	107

Table 3 Details of DOE runs with 2_V^{5-1} fractional factorial design

Std order	Oxygen flow	Hydrogen flow	Powder feed	Stand-off	SFM
1	570	1330	28	152	107
2	650	1330	28	152	61
3	570	1430	28	152	61
4	650	1430	28	152	107
5	570	1330	48	152	61
6	650	1330	48	152	107
7	570	1430	48	152	107
8	650	1430	48	152	61
9	570	1330	28	203	61
10	650	1330	28	203	107
11	570	1430	28	203	107
12	650	1430	28	203	61
13	570	1330	48	203	107
14	650	1330	48	203	61
15	570	1430	48	203	61
16	650	1430	48	203	107

determined by the surface speed), which helps to get a uniform thickness of the coating deposited on specimens. The other process variables were kept unchanged in all spray runs, as listed in Table 4. Spray passes set for Almen strip in DOE runs were varied from 10 to 35 depending on deposition rate, i.e., coating thickness per pass. Minitab 15 Statistical Software was used to organize DOE spray runs, analyze the experimental data, and obtain a fitting model which describes the response with process variables.

2.3 Preparation for Microstructure

Coated specimen for microstructure observation was cross sectioned by diamond blade, hot mounted, and ground and polished by an automatic grinder and polisher. Coating microstructure was observed using Leica DMILM microscope.

3. Results

3.1 Effect of Process Parameters on Residual Stress

The net deflections of coated Almen strips obtained in all DOE runs were all positive between 0.0178 and 0.312 mm, indicating that the final residual stress generated in the coating is compressive. In comparison with the acceptance limits of 0.076-0.30 mm required in AMS 2448, one spray run was over the limit, and two runs under the limit. Figure 1 shows the plot of Almen strip deflection vs. run order. The plot indicates that there is not a time sequence component affecting the response. With the 2_V^{5-1} fractional factorial experiment, a theoretical model for the response of Almen strip deflection was established by the Minitab Software, which contained a constant term, five main effect terms and ten two-factor interaction terms. The detailed information of the fitted theoretical model is listed in Table 5. The model can reveal the impact significance of all the terms in response to Almen strip deflection. More importantly, the fitted model can be used to predict the Almen strip deflection of the coating sprayed in any parameter setting selected or used to optimize the response. Pareto chart of effects for Almen strip deflection is shown in Fig. 2, which visually illustrates the significance of each term. It is found that most important factor to impact the response is stand-off distance, following by two-factor interaction of oxygen flow with hydrogen flow, surface speed, and then two-factor interaction of oxygen flow with powder FR.

The averages of Almen strip deflections obtained in DOE runs at low level and high level for each factor are displayed in Fig. 3. The solid horizontal line in the plots is the mean of all DOE experimental results. The slope of the line connecting the mean of response at low and high level indicates the impact significance of each main effect to the response. Apparently, the line in the stand-off distance plot has the steepest slope.

Table 4 Process variables fixed in DOE runs

Process variables	Conditions
Cooling	80 psi, compressed air
Substrate preheat	No preheat
Surface conditioning	Automatically grit blasted with 60 grit alumina
Carrier gas flow	57 SCFH
Nozzle	6.35 mm diameter × 228 mm length

Table 5 Coefficients for Almen strip deflection in fitted model using data in uncoded units

Terms	Coefficients
Constant	−10.8839
Oxygen flow	0.0208111
Hydrogen flow	0.0103234
Powder FR	−0.00122910
Stand-off	−0.0215924
SFM	−0.0129256
Oxygen flow × hydrogen flow	−1.80156E−05
Oxygen flow × powder FR	3.77031E−05
Oxygen flow × stand-off	1.32292E−05
Oxygen flow × SFM	7.41168E−06
Hydrogen flow × powder FR	−1.81125E−05
Hydrogen flow × stand-off	7.10294E−06
Hydrogen flow × SFM	3.72283E−06
Powder FR × stand-off	1.92892E−05
Powder FR × SFM	−4.80978E−06
Stand-off × SFM	1.48870E−05

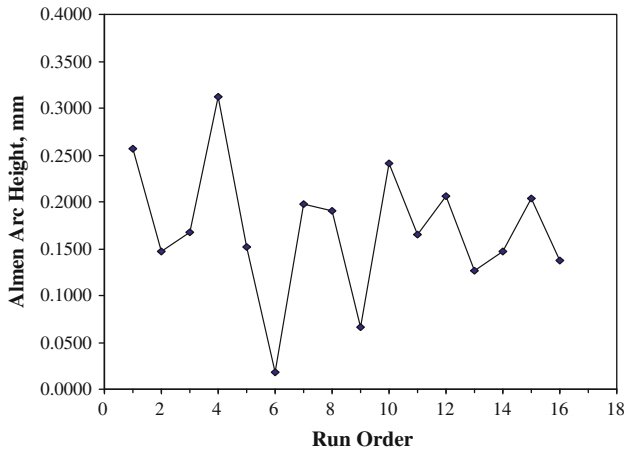

Fig. 1 Almen strip deflection vs. run order

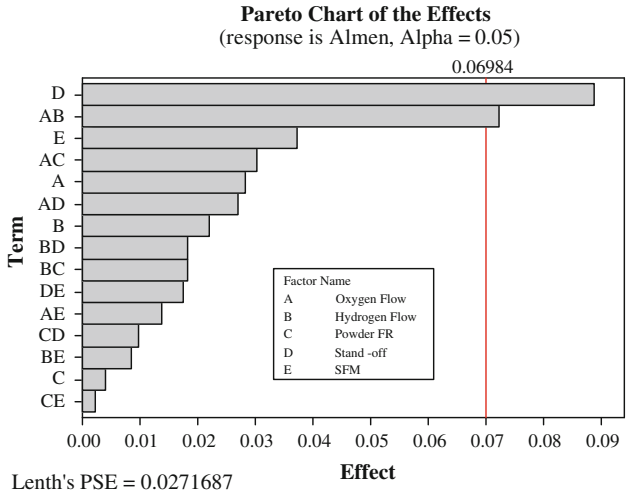

Fig. 2 Pareto chart of the standard effects for Almen strip deflection

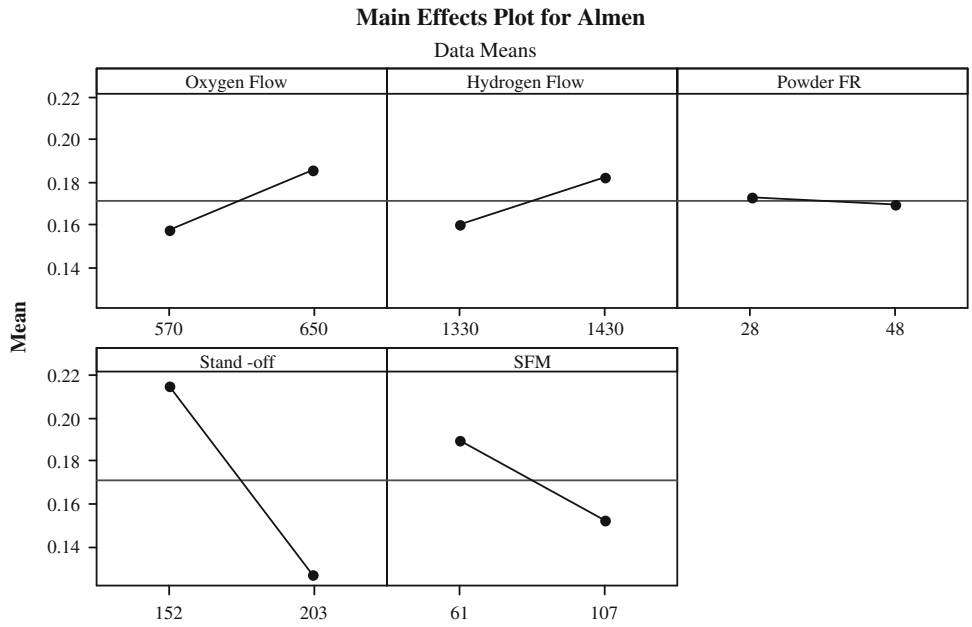

Fig. 3 Main effect plot for Almen strip deflection of coating

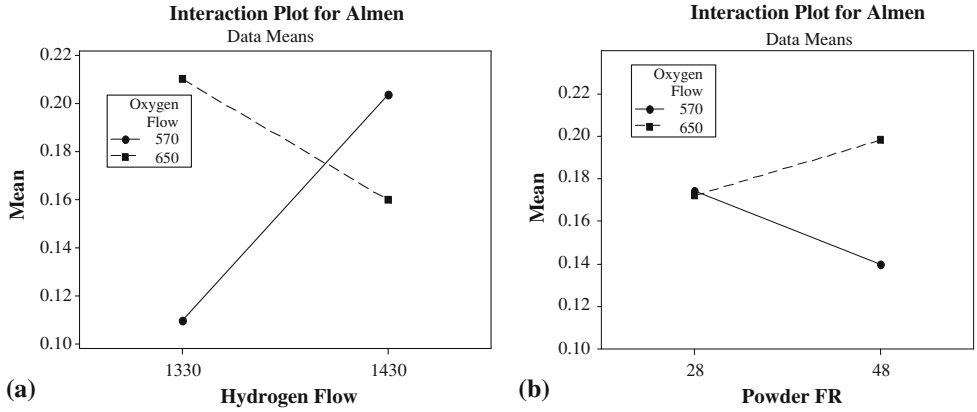

Fig. 4 Interaction plots for Almen strip deflection of coating: (a) interaction of oxygen flow with hydrogen flow; (b) interaction of oxygen flow with powder feed

It indicates that the stand-off distance has a greatest effect on the Almen strip deflection among the five main effects. The powder FR has a lowest effect on Almen strip deflection. In addition, it is seen that higher deflections of Almen strip will be obtained when the coating is sprayed at low level of stand-off distance and surface speed, and at high level of hydrogen flow and oxygen flow.

An interaction plot can be used to reveal the impact that changing the settings of one factor has on another factor. In Fig. 2, two terms of two-factor interaction considerably affect the response. The two-factor interaction plots are shown in Fig. 4. In Fig. 4(a), deflection of Almen strip obtained is much greater at high level of hydrogen flow than at low level when oxygen flow is at low level; however, an opposite result will happen when oxygen flow is at high level. Figure 4(b) indicates that powder FR at high level increases the deflection of Almen strip when oxygen flow is at high level; on the other hand, it decreases the deflection when oxygen flow is at low level.

3.2 Relationships Between Deflection of Almen Strip and In-Process Measurements

Velocity and temperature of in-flight particle in flame, as well as substrate temperature, were measured in DOE spray runs. The relationships between the measurements and deflection of Almen strip were summarized, and will be used to interpret the effect of factors on residual stress in the coating. The velocity of in-flight particle in flame measured was varied from 580 to 640 m/s, and the temperature from 1815 to 2045 °C in all DOE runs. When taking the velocity and temperature as responses, and oxygen flow, hydrogen flow, and power FR as factors, with statistical analysis by using Minitab Statistic Software, it is found that: oxygen and hydrogen gas flows significantly increase velocity of in-flight particle; oxygen flow significantly increases in-flight particle temperature; and powder FR at high level will reduce velocity and temperature of in-flight particle.

In the current DOE spray runs, there were two stand-off distances used, 152 and 203 mm. Therefore, when the spray is run at the stand-off distance of 203 mm, the measurements are not the actual impingement velocity and temperature of in-flight particle at the moment the particle impinges the substrate. Some existing studies have found that the variation of velocity and temperature of in-flight particle in flame is limited at the distance within 100-200 mm in HVOF WC-Co spray (Ref 20, 21). In this study, one experiment was conducted to measure the velocity and temperature of in-flight particle in flame with changing stand-off distance, as shown in Fig. 5. The measurement indicates that the differences in velocity and temperature at 152 and 203 mm are only 8 m/s and 16 °C. At the stand-off distance of 203 mm, the impingement velocity and temperature of in-flight particle in flame may be attained by adjusting these differences to the measurements obtained in DOE runs. The adjusted impingement velocity and temperature are not real measurement, but they should be of enough exactness for qualitative discussion in this study.

Figure 6 comprises scatter plots showing the relationships between deflection of Almen strip and impingement velocity and temperature of in-flight particle in flame. In general, there exists a trend in Fig. 6(a) that the deflection of Almen strip increases with increasing the particle velocity. Although not quite clear, the variation of the deflection with particle temperature seems to have the same trend as velocity except one point at 1827 °C. It indicates that the residual stress in the HVOF-sprayed WC-10Co-4Cr coating is proportional to the velocity and temperature of in-flight particle in flame. Figure 7 shows the scatter plot of Almen strip deflection with substrate temperature. A trend is also found that Almen strip deflection, i.e., residual stress in the coating, increases with substrate temperature.

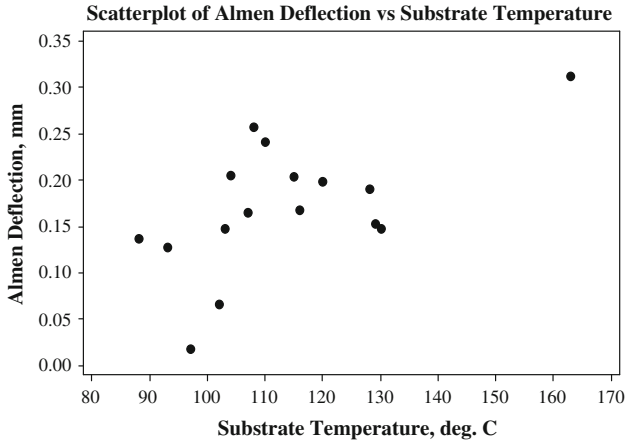

Fig. 7 Almen strip deflection vs. substrate temperature

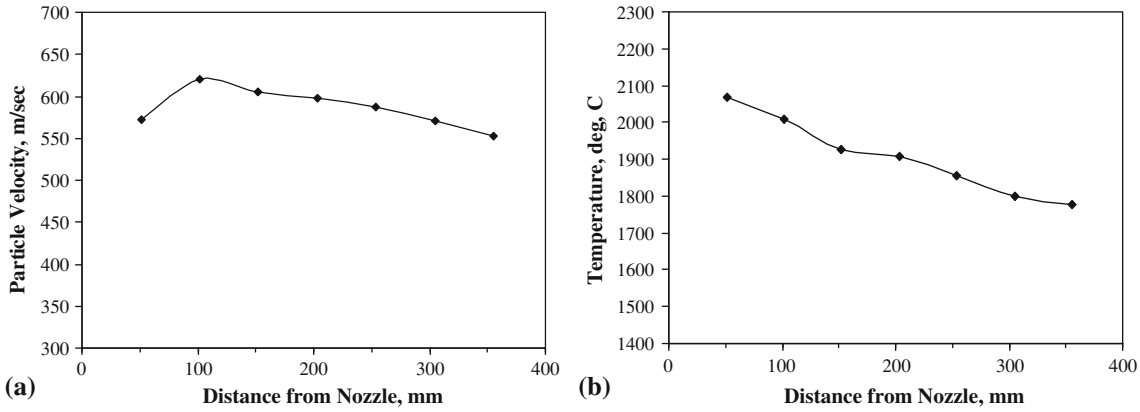

Fig. 5 Variations of velocity and temperature of in-flight particle in flame with distance from nozzle: (a) velocity and (b) temperature

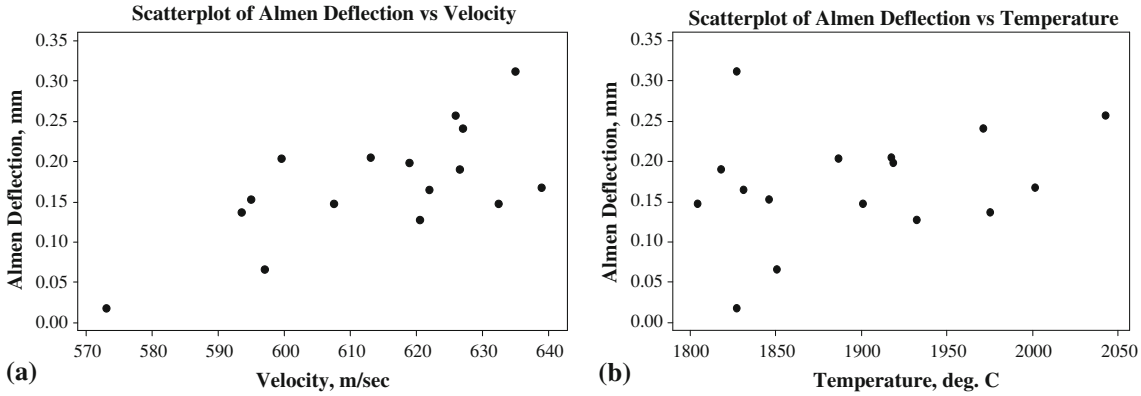

Fig. 6 Relationships between Almen strip deflection and particle velocity and temperature in flame: (a) Almen deflection and velocity; (b) Almen deflection and temperature

4. Discussion

4.1 Stress Type in the Coating

For HVOF thermal spray, it has been reported that the effects from peening, quenching, and mismatch of coefficient of thermal expansion between coating and substrate generate residual stress in coatings (Ref 15, 22, 23). Individual molten or partially molten droplets (particles) impinge a substrate or pre-deposited coating layer at high speeds, for instance, up to 640 m/s in this study. The impingement at this speed will cause plastic deformation on the pre-existing material surface, and a compressive residual stress will be induced in the coating. This "peening stress" is represented by σ_p. For WC-10Co-4Cr powder, only matrix materials Co and Cr are melted in HVOF flame, while WC remains in solid state. The solid WC will enhance the peening effect.

During HVOF spray, particle impinges the substrate or pre-deposited coating layer and forms a thin splat, which undertakes a rapid solidification and is cooled down to substrate temperature. In this short period, solidification and thermal contraction in the splat are restrained by substrate or pre-existing coating layer, thereby a quenching tensile stress in the individual splat is created (Ref 15, 24). The quenching stress in the splat can be estimated by an equation, as referred in the previous article (Ref 15):

$$\sigma_q = \alpha_c(T_m - T_s)E_c \quad \text{(Eq 2)}$$

where σ_q is quenching stress, α_c is the thermal expansion coefficient of the coating, T_m is the melting temperature of the coating, T_s is the substrate temperature, and E_c is the elastic modulus of the coating. The quenching stress in the splat is related to its elastic modulus and substrate temperature. In addition, the elastic modulus of the coating may be varied with process parameters because some chemical reactions may take place at a high temperature, causing a change of ingredients in the coating. The quenching stress in the splat could be reduced by metallurgical defaults in the coating such as crack, void, and interface separation, and material local plastic flow and creep.

Because of the mismatch in coefficients of thermal expansion (CTEs) of coating and substrate, a cooling stress, σ_c, will be generated in a coating when cooling to room temperature post thermal spraying. The type of stress depends upon CTE value of the coating and the substrate used. The cooling stress is proportional to the difference of CTEs between the coating and the substrate, as well as substrate temperature. In this study, the most content in the coating is WC having a very low CTE. The CTE of WC-10Co-4Cr coating is estimated at 6.5×10^{-6}/°C by the rule of mixtures (ROM) based on the nominal chemical composition of the powder. While, CTE of the Almen strip used material, SAE 1070, is 11.6×10^{-6}/°C. Obviously, the coating has a much lower CTE than the substrate, and a compressive cooling stress will be generated in the coating.

In the present system, the three types of stress described above, two compressive and one tensile, will determine the final residual stress σ_r in the coating, which is simply described as

$$\sigma_r = \sigma_p(\text{compressive}) + \sigma_q(\text{tensile}) + \sigma_c(\text{compressive}) \quad \text{(Eq 3)}$$

Any effect to induce more peening and cooling stresses, and less quenching stress will enhance the compressive residual stress in the coating.

4.2 Effect of Each Type of Stress on Residual Stress in the Coating

The velocity of in-flight particle in flame is one important factor to affect peening stress in the coating. In shot peen process, in which a compressive stress is generated on part surface, shot velocity will determine peening stress. The same principle should be applied to HVOF-spraying process. Higher impingement velocity of in-flight particle in flame will produce more peening stress in the coating, thus increasing the compressive residual stress in the coating. Figure 4(a) provides the evidence to support this standpoint. The similar result has been reported for TiO_2 powder in HVOF spray (Ref 16).

One can expect that higher impingement temperature of in-flight particle will cause higher substrate temperature because more heat will be transferred to the substrate from particle. The scatter plot between substrate temperature and impingement temperature of in-flight particle obtained in DOE runs is illustrated in Fig. 8, where no clear trend is seen. In the present DOE sprays, the substrate temperature depends not only on in-flight particle temperature, but also on deposition rate and surface speed (rotation speed and torch traverse speed). Based on Eq 2, a higher substrate temperature of T_s will lessen the quenching stress, and therefore strengthen the final compressive residual stress in the coating. In WC-10Co-4Cr powder, the matrix materials, such as Co, has a high melting temperature, T_m, at about 1500 °C, whereas T_s measured is only 10^2 orders of magnitude. In addition, the variation of T_s in all DOE runs is less than 100 °C. Hence, the value of $(T_m - T_s)$ only has a relatively small change. As a result, the change in T_s in this study applies a very limited effect on quenching stress in the coating. In general, as shown in Fig. 4(b), temperature of in-flight particle tends to increase the compressive residual stress in the coating in statistic viewpoint.

Microstructure observation by optical microscope indicates that there are no cracks and interfacial separation found in the coating in all DOE runs. Figure 9 illustrates the typical microstructures of the coating deposited at low and high particle temperature. In the figure, small gray particulates are WC; bright area is Co, and Cr metal matrix; pores are dark spot, and string oxides are shown by arrows. In general, the coating sprayed at high in-flight particle temperature contains more oxides/pores. The defects, especially pores, will result in the relaxation of quenching stress, thereby reducing quenching

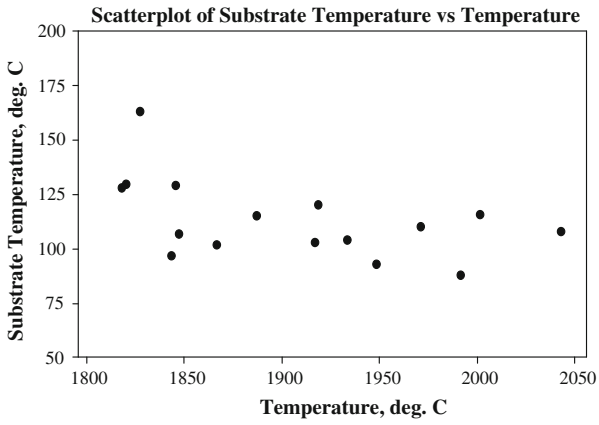

Fig. 8 Variation of substrate temperature with in-flight particle temperature in flame

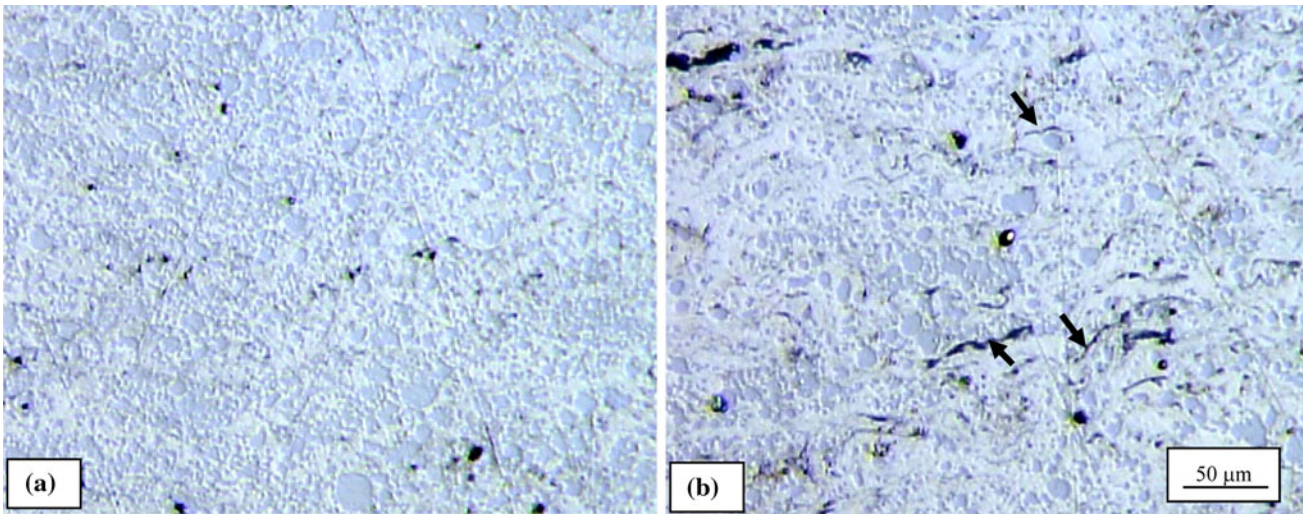

Fig. 9 Typical microstructures of coating deposited at low and high particle temperatures: (a) low particle temperature at 1815 °C; (b) high particle temperature at 2045 °C: arrows indicating oxide stringers

stress level in the coating. In addition, the volume of WC in the coating obtained at high in-flight particle temperature is less than that at low particle temperature because more WC is decarburized in high temperature flame. The degradation of WC occurring in HVOF WC-Co spray has been widely studied (Ref 5-7). In the case of a composite material, the linear ROM can be simply used to estimate the elastic modulus of the material (Ref 25). The reduction in the amount of WC in the coating will reduce elastic modulus of the coating because WC has a much greater elastic modulus than other matrix materials. In Eq 2, the decrease in E_c will result in low quenching stress. Therefore, at high in-flight particle temperature, the relaxation of quenching stress in the coating and reduction of elastic modulus of the coating shall be the reasons to cause a higher final compressive residual stress in the coating.

For the cooling stress, except to the difference of CTE of two materials, substrate temperature is another factor to impact cooling stress in the coating. The higher the temperature of substrate post spraying, the greater the cooling stress caused, which will increase the compressive residual stress in the present coating. This can be supported by Fig. 7. It should be noted that the change in microstructure of the coating discussed above may change the CTE value of the coating, thus affecting the cooling stress.

The above discussion generally described the influence of impingement velocity and temperature of in-flight particle in flame, and substrate temperature on the final compressive residual stress in the coating. The process parameters designated in DOE will impact the three types of stress in different ways. The amounts of three types of stress in Eq 3 are varied from one DOE run to another. In a process parameter setting of DOE run, a change in one parameter may enhance some type stress, but any change in another may reduce some ones. This is why somewhat big scatter distributions are seen in the plots of Fig. 6, 7, and 8.

One abnormal point at low particle temperature of 1827 °C in Fig. 6(b) has a big deflection of Almen strip. In this spray run, there was a measurement of high substrate temperature post spraying. Cooling stress contributed by the high substrate temperature dominates the final residual stress in the coating and produce the high value of the stress.

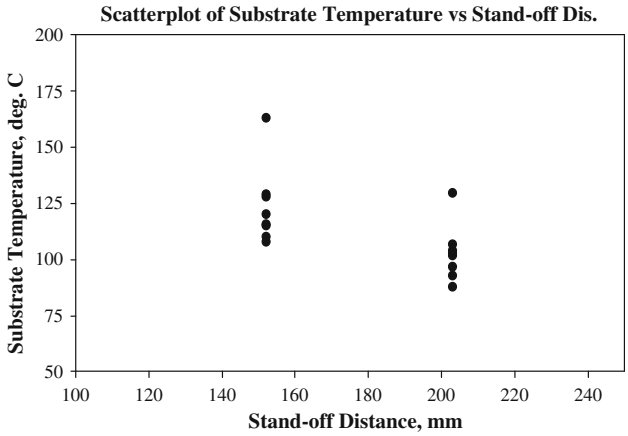

Fig. 10 Substrate temperature vs. stand-off distance

4.3 Effect of Process Parameters on Residual Stress in the Coating

In-flight particle velocity and temperature in flame, and substrate temperature depend on process parameters in HVOF spraying. In Fig. 1, the stand-off distance is the most important factor to affect Almen strip deflection, i.e., residual stress. In Fig. 2, Almen strip deflection is significantly greater at low level of stand-off distance than at high level. According to the measurement as shown in Fig. 5, the particle velocity in flame at low level stand-off distance of 152 mm is somewhat more than that at high level stand-off distance of 203 mm. Higher particle velocity will result in greater peening stress in the coating. The relationship between substrate temperature and stand-off distance is shown in Fig. 10. In common sense, the low level of stand-off distance will result in higher substrate temperature post spraying, thereby producing more cooling stress in the coating. Those two effects cause much greater compressive residual stress in the coating sprayed at low level stand-off distance than at high level stand-off distance. High level of oxygen flow increases particle temperature in flame, which somewhat reduces quenching stress in coating splat. Also high level oxygen flow increases velocity of in-flight

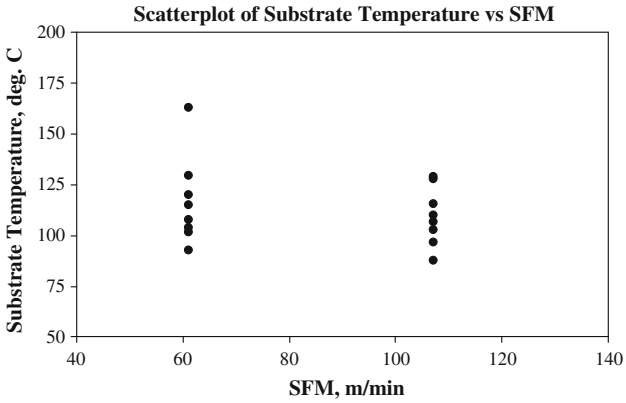

Fig. 11 Substrate temperature vs. surface speed

particle in flame, strengthening peening stress. Hence, both of these enhance the compressive residual stress in the coating. Hydrogen flow at high level tends increasing the compressive residual stress in the coating since more peening stress is produced in the coating by higher velocity of in-flight particle in flame. Figure 11 indicates substrate temperature at low and high level of surface speed. The two group readings are not much different, but it still looks that the former is relatively higher than the latter. This is one root that the coating will get more compressive residual stress at low level surface speed than at high level because of more cooling stress generated in the coating. In addition, another possible comprehension on it is that the substrate temperature at low level surface speed is greater than that at high level, which strengthens cooling stress in the coating, because more heat can be transferred to the substrate with low traverse torch speed.

In Fig. 4(a), in the condition of low level oxygen flow, high level hydrogen flow increases in-flight particle velocity in flame and it is beneficial for peening stress, resulting in higher compressive residual stress in the coating. At high level of oxygen flow, high level hydrogen flow decreases in-flight particle temperature in flame. It reduces pore/oxide content in microstructure of the coating and improves elastic modulus of the coating. These strengthen quenching stress in individual coating splat, thereby reducing the compressive residual stress in the coating.

In Fig. 4(b), in the condition of low level of oxygen flow, high level of powder FR reduces the compressive residual stress in the coating because velocity of in-flight particle in flame is lower at high level of powder FR than at low level, thus reducing the peening stress in the coating. At high level of oxygen flow, the compressive residual stress in the coating somewhat increases at high level of powder FR probably due to higher substrate temperature, which increases cooling stress in the coating, because more heat is transferred to the substrate by more powder deposit.

5. Conclusion

In this study, based on two-level fractional factorial DOE, 2_V^{5-1}, with five process variables as factors, the compressive residual stress in HVOF-sprayed WC-10Co-4Cr coating was studied. A theoretical model for the compressive residual stress in the coating with the process variables was fitted by a statistic software. Three types of stress generated in HVOF spraying were discussed based on experimental measurements obtained in DOE runs. Stand-off distance is the most important factor to impact the compressive residual stress in the coating. At a low level stand-off distance, higher velocity of in-flight particle in flame and higher substrate temperature post spraying contribute more peening and cooling stresses, resulting in greater compressive residual stress in the coating. Higher temperature of in-flight particle in flame at high level oxygen flow results in more pore/oxide in microstructure it also which relaxes tensile quenching stress in the splat, and lowers elastic modulus of coating material due to less WC in the coating which reduces quenching stress. These effects result in more compressive residual stress in the coating. Hydrogen flow at high level significantly increases velocity of in-flight particle in flame, enhancing peening stress, thus increasing the compressive residual stress in the coating.

References

1. B. Startwell, Thermal Spray Coatings as Alternative to Hard Chrome Plating, *Weld. J.*, 2000, **79**, p 39–43
2. D. Lee, R. Eybel, and R. Evans, Development and Implementation of HVOF WC/Co/Cr Coating as Alternative to Electrolytic Hard Chrome Plate in Landing Gear Applications Using Natural Gas as Fuel, *Thermal Spray 2003: Advancing the Science and Applying the Technology*, ASM International, 2003, p 371–376
3. R. Evans, R. Panza-Giosa, E. Cochien, and S. Maitland, HVOF-Applied WC-Co-Cr as a Hard Chrome Replacement for Landing Gear, *Thermal Spray 2006: Science, Innovation, and Application: Proceedings of the Spray Conference*, ASM International, 2006, p 615–617
4. P.F. Ruggiero, Tungsten Carbide Coatings Replace Chromium, *Adv. Mater. Process.*, 2005, **163**(7), p 39–40
5. R. Schwetzke and H. Kreye, Microstructure and Properties of Tungsten Carbide Coatings Sprayed with Various High-Velocity Oxygen Fuel Spray Systems, *J. Therm. Spray Technol.*, 1999, **8**, p 433–439
6. J.M. Guilemany, S. Dosta, J. Nin, and J.R. Miguel, Study of the Properties of WC-Co Nanostructured Coatings Sprayed by High-Velocity Oxyfuel, *J. Therm. Spray Technol.*, 2005, **14**, p 405–413
7. J.G. Legoux, S. Bouaricha, and J.P. Sauer, Cracking and Spalling Behavior of WC-17%Co Cermet Coatings, *Thermal Spray 2006: Science, Innovation, and Application: Proceedings of the Spray Conference*, ASM International, 2006, p 609–661
8. A. Ghabchi, T. Varis, E. Turunen, T. Suhonen, X. Liu, and S.P. Hannula, Behavior of HVOF WC-10Co-4Cr Coatings with Different Carbide Size in Fine and Coarse Particle Abrasion, *J. Therm. Spray Technol.*, 2010, **19**, p 368–377
9. L. Prchlik, S. Sampath, J. Gutleber, G. Banche, and A.W. Ruff, Friction and Wear Properties of WC-Co and Mo-Mo_2C Based Functionally Graded Materials, *Wear*, 2001, **8**, p 1103–1115
10. M.Y.P. Costa, M.L.R. Venditti, H.J.C. Voorwald, M.O.H. Cioffi, and T.G. Cruz, Effect of WC-10%Co-4%Cr on the Ti-6Al-4V Alloy Fatigue Strength, *Mater. Sci. Eng.*, 2009, **507 A**, p 29–36
11. A.K. Maiti, N. Mukhopadhyay, and R. Raman, Improving the Wear Behavior of WC-CoCr-Based HVOF Coating by Surface Grinding, *J. Mater. Eng. Perform.*, 2009, **18**, p 1060–1066
12. J.C. Tan, L. Looney, and M.S.J. Hashmi, Residual Stress Analysis of WC-Co Solid Components Formed by HVOF Thermal Spraying Process, *Proc. Adv. Powder Metall. Part. Mater. Wash. DC*, 1996, **3**, p 941–952
13. J. Stokes and L. Looney, Residual Stress in HVOF Thermally Sprayed Thick Deposits, *Surf. Coat. Technol.*, 2004, **177–178**, p 18–23
14. J.P. Sauer and P. Sahoo, HVOF Process Control Using Almen and Temperature Measurement, *Thermal Spray 2001: New Surface for a New Millennium: Proceedings of the International Thermal Spray Conference*, ASM International, 2001, p 791–796
15. J. Stokes and L. Looney, Properties of WC-Co Components Produced Using the HVOF, *Thermal Spray Process, Proceedings of 2000 Thermal Spray Conference*, ASM International, 2000, p 263–271
16. M. Gaona, R.S. Lima, and B.R. Marple, Influence of Particle Temperature and Velocity on the Microstructure and Mechanical

Behavior of High Velocity Oxy-Fuel (HVOF)-Sprayed Nanostructured Titania Coatings, *J. Mater. Process. Technol.*, 2008, **198**, p 426–435
17. J. Matejicek and S. Sampath, In Situ Measurement of Residual Stresses and Elastic Moduli in Thermal Sprayed Coatings: Part 1: Apparatus and Analysis, *Acta Mater.*, 2003, **51**, p 863–872
18. S. Sampath, V. Sirnivasan, A. Valarezo, A. Vaidya, and T. Streibl, Sensing, Control, and In Situ Measurement of Coating Properties: An Integrated Approach Toward Establishing Process-Property Correlations, *J. Therm. Spray Technol.*, 2009, **18**, p 243–255
19. O.C. Brandt, Measuring of Residual Stresses in Thermal Sprayed Coatings, *Proceeding of Eight National Thermal Spray Conference 1995* (Texas, USA), 1995, p 451–455
20. L. Zhao, M. Maurer, F. Fischer, and E. Lugscheider, Study of HVOF Spraying of WC-CoCr Using On-line Particle Monitoring, *Surf. Coat. Technol.*, 2004, **185**, p 160–165
21. J.P. Sauer and M. Carroll, Thermal Spray Process Training—A New Perspective, *International Thermal Spray Conference & Exposition 2009*, 4–7 May (Las Vegas, USA), 2009
22. S. Kuroda, Y. Tashiro, H. Yumoto, S. Taira, H. Fukanuma, and S. Tobe, Peening Action and Residual Stress in High-velocity Oxygen Fuel Thermal Spraying of 316L Stainless Steel, *J. Therm. Spray Technol.*, 2001, **10**, p 367–374
23. J. Stokes and L. Looney, Predicting Quenching and Cooling Stresses within HVOF Deposits, *J. Therm. Spray Technol.*, 2008, **17**, p 908–914
24. T.W. Clyne, Residual Stresses in Coated and Layered Systems, *Encyclopaedia of Materials: Science and Technology—Elasticity and Residual Stress*, P.J. Withers, Ed., Elsevier, 2001, p 8126–8134
25. D.J. Lloyd, Particle Reinforced Aluminum and Magnesium Matrix Composites, *Int. Mater. Rev.*, 1994, **39**, p 1–23